Burning Velocity Measurements in Aluminum-Air Suspensions Using Stabilized Dust Flames.

Samuel Goroshin, Massimiliano Kolbe, and John Lee
McGill University, Montreal, Quebec, Canada
e-mail: sam@mecheng.mcgill.ca

Introduction.

Laminar burning velocity (sometimes also referred in literature as fundamental or normal flame propagation speed) is probably the most important combustion characteristic of the premixed combustible mixture. The majority of experimental data on burning velocities in gaseous mixtures was obtained with the help of the Bunsen conical flame [1]. The Bunsen cone method was found to be sufficiently accurate for gaseous mixtures with burning velocities higher than 10-15 cm/s at normal pressure [1,2]. Hans Cassel [3] was the first to demonstrate that suspensions of micron-size solid fuel particles in a gaseous oxidizer can also form self-sustained Bunsen flames. He was able to stabilize Bunsen flames in a number of suspensions of different nonvolatile solid fuels (aluminum, carbon, and boron). Using the Bunsen cone method he estimated burning velocities in the premixed lean aluminum-air mixtures (particle size less than 10 microns) to be in the range of 30-40 cm/s. Cassel also found, that the burning velocity in dust clouds is a function of the burner diameter [4]. In our recent work [5], we have used the Bunsen cone method to investigate dependence of burning velocity on dust concentration in fuel-rich aluminum dust clouds. Burning velocities in stoichiometric and fuel-rich aluminum dust suspensions with average particle sizes of about 5 microns were found to be in the range of 20-25 cm/s and largely independent on dust concentration. These results raise the question to what degree burning velocities derived from Bunsen flame specifically and other dust flame configurations in general, are indeed fundamental characteristics of the mixture and to what degree are they apparatus dependent. Dust flames in comparison to gas combustion, are thicker, may be influenced by radiation heat transfer in the flame front, respond differently to heat losses [6], and are fundamentally influenced by the particular flow configuration due to the particles inertia. Since characteristic spatial scales of dust flames are larger, one can expect that they will also be more sensitive than homogeneous combustion to a particular experimental geometric configuration of the flame and the flow. With such sensitivity the introduction of the very concept of the fundamental flame speed may be problematic for dust combustion. With this in mind, the objective of the present work is to further investigate Bunsen dust flames and evaluate to what degree do burning velocities derived from Bunsen cone depend on experimental conditions (i.e. flow rate and nozzle diameter).

Experimental Details.

<u>*Dust Burner.*</u>
The general schematic of the experimental “dust burner” set-up is shown in Fig. 1A. The details of the experimental set-up and principles employed in the dust dispersion system are described in our previous works [5,6]. The following description will only specify important modifications that were made to the apparatus in accordance with the objectives of the present work. A simple conical nozzle replaced the water-cooled detached ring that was used previously to stabilize dust flames [5]. The use of the flame stabilized directly on the nozzle, instead of the detached ring, eliminates the uncertainty in flow rate that might result from gas entrainment into the flame from the surrounding atmosphere. With the flame anchored on the nozzle the dust concentration is monitored directly within the dust supply tube by the redesigned laser light extinctiometer (Fig. 1C). In this modified design, the light emitted by the 3 mW laser diode is introduced into the dust tube through the airflow protected windows, it then passes through narrow channel and is focused by a long focal lens on a small aperture (d= 0.25 mm). The aperture plays the role of a spatial filter that cuts scattered laser light thus making deviation from the Bouguer’s light attenuation law negligible even for optically thick dust clouds. A narrow bandwidth interference filter permits only the laser light to pass, protecting the photodetector from the light emitted by the flame and scattered by aluminum particles. The signal from the photodetector is amplified and recorded by a computer data acquisition system.

The gas dispersing flow is maintained constant throughout the duration of an experiment, and variation of the dust concentration is achieved by varying the dust feeding rate. In order to regulate the dust flow rate through the nozzle, an ejection system is used to eject part of the flow from the main stream into a bypass tube. Pure nitrogen is used as an ejecting gas. Thus the flow removed from the main stream by the ejector can be easily calculated by measuring the concentration of oxygen in the bypass tube. Oxygen concentration in the ejector flow is continuously monitored by an in-line electrolytic oxygen analyzer and is recorded by a computer data acquisition system.

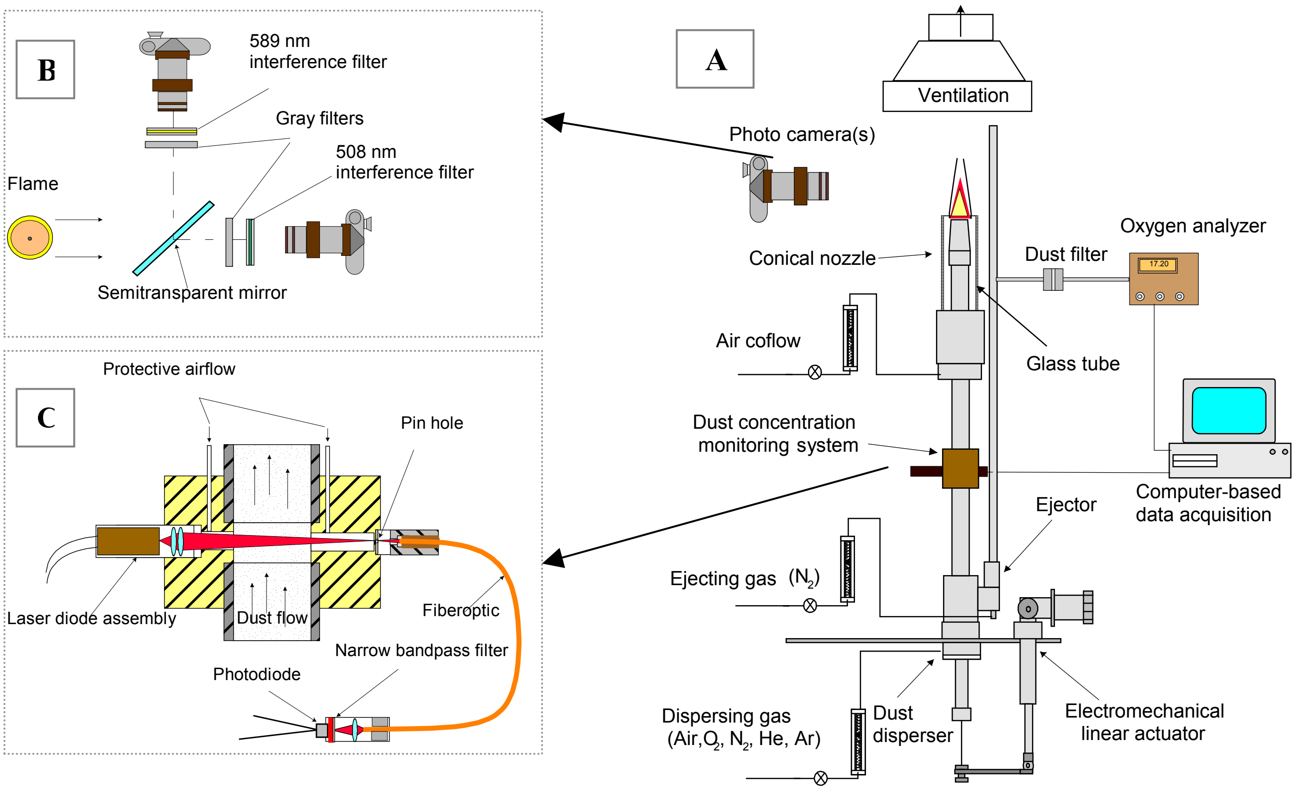

Figure 1. General schematic of the experimental "dust burner" set-up (A), schematic of the photographic arrangement (B) and the schematic of the laser light extinctiometer for monitoring the dust concentration (C).

Aluminum powder.

Atomized aluminum powder (Ampal 637, Ampal Inc., NJ) used in these experiments was from the same batch as in our previous works on flame quenching distance measurements [6] and flame speed measurements in rich mixtures [5]. The powder's aluminum content is no less than 99.5% and the aluminum particles are of a spheroidal or nodular shape. Differential distribution of particle sizes in the powder is shown in Fig. 2.

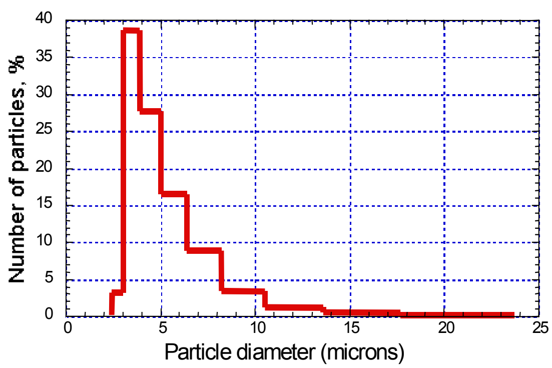

Figure 2. Particle size distribution in aluminum powder.

Dust concentration measurements.

The laser light extinctiometer was calibrated by the complete aspiration of dust from the nozzle flow through a set of filters with a vacuum pump for a known time. Dust mass concentration in the flow is then determined by dividing total mass of the aspired dust by the volume of the gas passing through the nozzle during the same time. The calibration curve for the light extinctiometer is shown in Fig. 3.

Mean particle Sauter diameter (d_{32}) in a suspension can be calculated from the data shown in Fig. 3 by using Bouger's light attenuation law. The calculations indicate an average particle diameter of about 6 μm (due to diffraction, light attenuation cross section for particles of this size is twice the size of the particle cross section [7]). This value practically coincides with the average Sauter diameter derived from the particle size distribution shown in Fig. 2 (d_{32} = 5.8 μm), which confirms that the particle agglomeration in the dust flow is negligible.

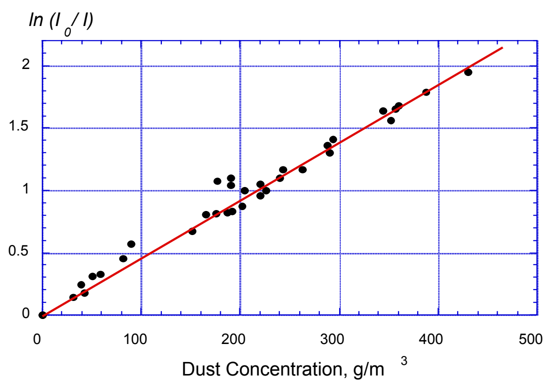

Figure 3. Calibration curve for the light extinctiometer.

Photographic arrangement.

The flame image was split by a semitransparent mirror as is shown in Fig. 1B and simultaneously recorded by two single-lens Canon reflex cameras through two different narrow bandwidth interference filters. The bandwidth of one filter coincides with the sodium D-line (589 nm) and the bandwidth of the other coincides with the edge of the green band in the AlO molecular spectrum (508 nm). As the sodium concentration in flame remains constant, the maximum intensity in the sodium radiation might be associated with the maximum flame temperature, whereas the appearance of the AlO line indicates the ignition of aluminum particles. The flame images were digitized using a high-resolution slide scanner. The flame shapes and surface areas of the flame inner cones were determined with the help of image processing software.

Experimental Results.

General observations.

A photograph of the stoichiometric aluminum dust flame is shown in Fig. 4 along with a picture of a stoichiometric methane-air flame stabilized on the same nozzle at approximately the same flow rate (about 300 cm^3/s).

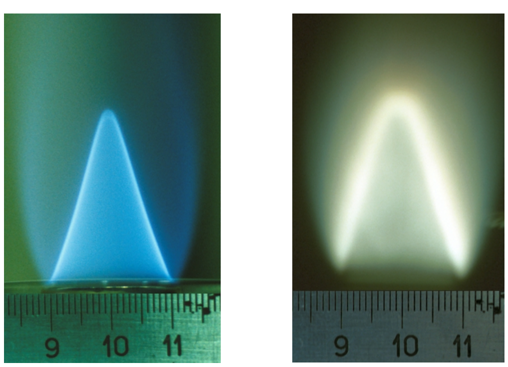

Figure 4. Photographs of the methane and aluminum stoichiometric flames stabilized on the same nozzle.

In comparison to the methane flame, the dust flame appears to be thicker and a bit larger. The flame base of the gas flame slightly overhangs the nozzle's rim, while the diameter of the base of the dust flame is closer to the inner diameter of the nozzle. The base of the dust flame is also lifted by about 2-3 mm above the nozzle exit while the distance from the nozzle to the base of the gas flame is less than 0.5 mm. The tip of the dust flame is more rounded and the inner boundary of the cone is usually better defined in comparison with the defused outer boundary. At very large dust concentrations the tip of the dust flame often opens up. The size of the opening is however relatively small (1-2 mm).

Comparison of the inner flame cone contours derived from the photos taken through 508 nm and 589 nm filters (Fig. 5) show that they practically coincide with the exception of a small region close to the tip of the flame. The burning velocities derived from these pictures differ by less than 5%; thus only flames filmed through the 508 nm filter were used to measure burning velocity.

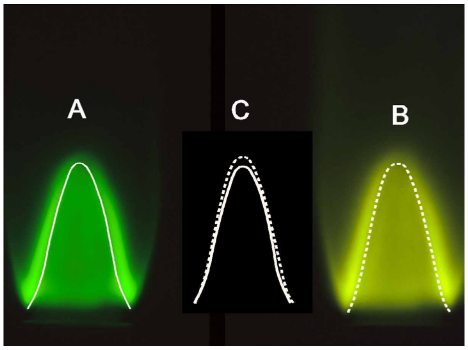

Figure 5. Pictures of aluminum-air flame taken through 508 nm (A) and 589 nm (B) interference filters. C- superimposed contours of the inner flame cones from pictures A and B.

Burning Velocity Measurements.

Conical cylindrical brass nozzles with exit diameters 14, 18, and 22 mm were used to stabilize aluminum dust flames at different flow rates. All nozzles have the same base diameter (24.5 mm) and height (60 mm). The dependence of the burning velocity on dust concentration at two different flow rates is shown in Fig. 6 for 18 mm nozzle.

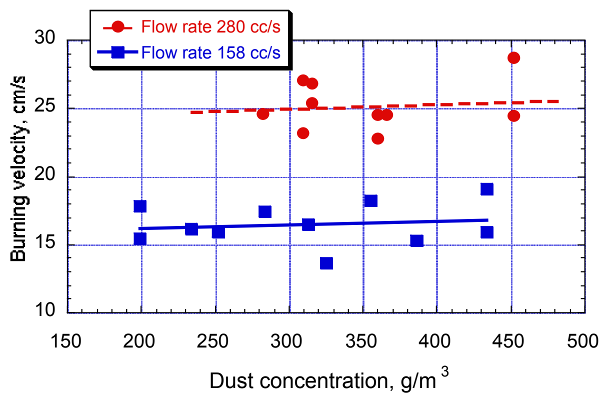

Figure 6. Dependence of burning velocity on dust concentration at two different flow rates (18 mm nozzle).

The present experiments confirm the result of our previous work [5] which shows that flame speed in rich aluminum suspensions is insensitive to dust concentration. Surprisingly, the burning velocity demonstrates also no noticeable decline in the range of dust concentrations below stoichiometry (200-300 g/m^3). The burning velocity shows clear tendency to increase with the increase in flow rate. The derived dependence of the burning velocity on flow rate at approximately uniform dust concentration (350 g/m^3) is shown in Fig. 7. Maximum flow rate at which flame ceases to be completely anchored at the nozzle exit prior to blowoff, is about 300 cm^3/s, whereas at flow rate below 150 cm^3/s the flame is prone to flashback for the 18-mm nozzle.

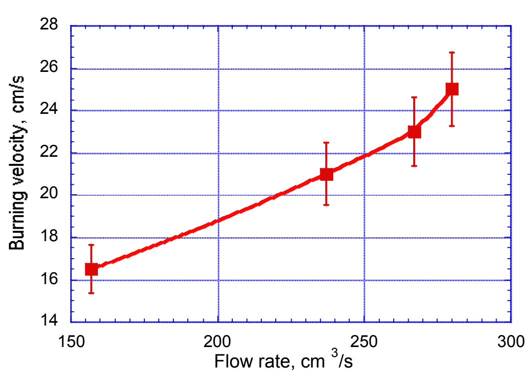

Figure 7. Dependence of the burning velocity on flow rate (18 mm nozzle, dust concentration is about 350 g/m^3).

In our experiments with different nozzle diameters, we were unable to stabilize flames on the large nozzle (22 mm) at the same flow rates as on 14 and 18 mm nozzles. Thus for the data shown in Fig. 8, the flow rates for two nozzles (14 mm and 18 mm) are the same (~ 250 cm^3/s) whereas for the 22 mm nozzle the flow rate is higher (~ 400 cm^3/s). Nevertheless, the results clearly show that burning velocity decreases with increase in the nozzle diameter. As was mentioned earlier, Cassel reported the same observation in his pioneering experiments with Bunsen dust flames [4].

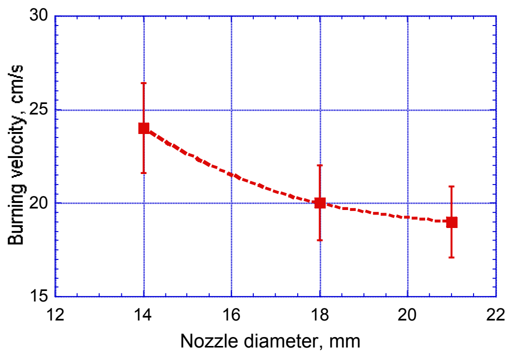

Figure 8. Dependence of the burning velocity on the nozzle diameter.

Discussion.

Cassel suggested [4] that the increase in the burning velocity for dust flames stabilized on smaller nozzles might be the result of the converging heat flux produced by flame curvature analogous to the known effect that increases the flame speed at the tip of the Bunsen gas flame [1]. According to the phenomenological theory pioneered by Markstein [8], the increase in the burning velocity due to the curvature effect is proportional to $(1+ \delta/R)$ (where R is the radius of the flame and δ is the flame thickness). Cassel speculated that due to the larger thickness of the dust flame the dust burning velocity might be effected even with a relatively small (compared to gas) flame curvature.

The width of hydrocarbon flames is typically less than 1 mm and is dominated by the flame preheat zone (also known as Markstein length). Due to the strong Arrhenius dependence of the reaction rate on temperature, the reaction zone in gas flames occupies only a small temperature interval below the adiabatic flame temperature. Thus the spatial thickness of the reaction zone in gas flames is negligible in comparison to the preheat zone. Unlike gas combustion, the combustion rate of dust particles after ignition is not controlled by Arhenius kinetics but is limited by the rate of oxygen diffusion towards the particle surface. The average flame temperature has little effect on the diffusion-controlled combustion rate. Thus the reaction zone in dust flames occupies a wide temperature interval that spans from the particle ignition temperature (about 2200 K for aluminum particles [9]) up to the adiabatic flame temperature (3500 K for the stoichiometric aluminum-air mixtures). Consequently, the spatial width of the dust combustion zone might be comparable or even exceed the width of the preheat zone (Markstein length) and the total width of the dust flame is essentially a sum of the preheat δ_p and combustion zones δ_c: $\delta=\delta_p+\delta_c$. Thus even if the Markstein lengths of the dust and gas flames are similar (comparable flame speeds), the total thickness of the dust flame is larger.

The thickness of aluminum dust flame can be estimated from quenching distance data. The flame quenching distances in aluminum-air suspensions have been measured by the authors in [6] using the same aluminum powder as in the present experiments. It was found that the quenching distance in fuel-rich aluminum-air mixtures is about 5 mm and does not depend on dust concentration. The simple flame quenching theory proposed by authors in the same work [6] predicts the ratio of the quenching distance to flame thickness to be about 1.8 for aluminum flames. Thus, the estimated flame thickness of the rich aluminum dust flame is about 2.8 mm with at least half of this length belonging to the combustion zone. We can now use the estimated flame thickness to calculate the burning velocity of the unperturbed flat flame S_u^o in accordance to the Markstein expression:

$$S_u^o = \frac{S_u}{\overline{A}}, \ \overline{A} = \overline{(1+\delta/R)} \tag{1}$$

Here S_u is the burning velocity of the curved flame calculated by dividing the dust flow through the nozzle by the total flame surface area and $\overline{A}$ is an average value of the flame thickness-to-flame radius ratio calculated separately for each flame shape. The flame curvature along the flame cone was averaged with the "weight" that is proportional to the ratio of the dust flowing through the flame segment of the given radius to the total dust flow through the burner:

$$\overline{1/R} = \frac{1}{H_0}\int_0^{H_0} \frac{1}{r(h)}\left(\frac{r(h)}{R_0}\right)^2 dh \tag{2}$$

Here H_0 is the flame height, R_0 is the radius of the flame base, and $r(h)$ is the second degree polynomial approximating the projection of the flame shape. Several flame profiles that represent different nozzle diameters and flow rates were carefully measured to calculate average values of the parameter $\overline{A}$ along the flame length. The results of the calculation of the burning velocity of the unperturbed flat flame (in accordance to expression (1)) are shown in Table 1.

Table 1 Calculations of the unperturbed burning velocity S_u^o for different flames.

Dust concentration (± 50 g/m^3)	Nozzle diameter (mm)	Flow rate (l/s)	Flame height, (mm)	S_u^o, (cm/s)
550	14.0	0.18	20	19.5
550	14.0	0.22	24	19.4
550	14.0	0.24	29	17.6
660	14.0	0.27	30	20.8
660	14.0	0.32	34	19.6
430	18.0	0.16	23	16.2
460	18.0	0.16	24	15.8
460	18.0	0.20	26	18.0
480	18.0	0.24	27	18.9
570	18.0	0.23	28	16.3
600	21.0	0.46	53	15.8
600	21.0	0.47	38	18.9
550	21.0	0.51	49	16.9
550	21.0	0.55	47	19.1
600	21.0	0.59	56	18.1
			$S_{u\ ave}^o$ =	**18.1±1.3 cm/s**

As can be seen from the Table 1, the unperturbed burning velocity is largely independent both on flow rate and nozzle diameter. Hence the previously observed scatter of the non-corrected burning velocities is simply an artifact of the dust flame curvature effect. The results obtained in this work prove that the Bunsen flame can remain as a valuable tool in obtaining fundamental flame parameters (burning velocity) also in dust flames, providing that the flame curvature effect as well as the stretch effect (when present) are taken into consideration.

***Acknowledgment**: The authors gratefully acknowledge the financial support received for this research from the Canadian Space Agency under the Microgravity Science Program.*

References.

1. B. Lewis and G. von Elbe, *Combustion and explosion of Gases*, , Academic Press, NY, 1987. 2. Andrews, G.E., and Bradley, D., "Determination of Burning Velocities: A Critical Review", *Comb. Flame* 18: 133-153, 1972.
3. Cassel, H. M., Das Gupta, A.K., Guruswamy, S., "Factors Affecting Flame Propagation Through Dust Clouds" *Proc. Comb. Inst.* 3: 185-190, 1949. 4. Cassel, H.M., *Some Fundamental Aspects of Dust Flames*, Report of Investigation No. 6551, US Bureau of Mines, 1964. 5. Goroshin, S., Fomenko, I., and Lee, J.H.S., "Burning Velocities in Fuel-Rich Aluminum Clouds", *Proc. Comb. Inst.* 26: 1961-1967, 1996. 6. Goroshin, S., Bidabadi, M., and Lee, G.H.S., "Quenching Distance of Laminar Flame in Aluminum Dust Clouds", *Comb. Flame* 105: 147-160, 1996. 7. Reist, P., *Aerosol Science and Technology,* McGraw-Hill, New York, 1993. 8. *Non-Steady Flame Propagation,* Ed. George H. Markstein, The Pergamon Press, New York, p.22 9. Fridman, R., and Macek, A., *Combust. Flame* 6: 9-19, 1962.